Scripta Materialia 142 (2018) 1–5

Contents lists available at ScienceDirect

Scripta Materialia

journal homepage: www.elsevier.com/locate/scriptamat

Regular article

Crystallographic study of plasticity and grain boundary separation in FeCo alloy using small single- and bi-crystalline specimens

Daichi Kishi, Tsuyoshi Mayama, Yoji Mine *, Kazuki Takashima

Department of Materials Science and Engineering, Kumamoto University, 2-39-1 Kurokami, Chuo-ku, Kumamoto 860-8555, Japan

ARTICLE INFO

Article history:
Received 16 May 2017
Received in revised form 17 July 2017
Accepted 8 August 2017
Available online xxxx

Keywords:
Micromechanical characterisation
Intermetallic compounds
Grain boundaries
Plastic deformation
Finite element analysis

ABSTRACT

To study the relationship between the plasticity and intergranular fracture of FeCo intermetallic alloys, small, single- and bi-crystalline specimens were subjected to micro-tensile testing and crystal plasticity finite element analyses. The single-crystalline specimens exhibited a high strength and a large strain-to-failure compared with the bi-crystalline and polycrystalline specimens. The critical resolved shear stress for the $\{1\bar{1}0\}\ \langle 111\rangle$ slip was ~100 MPa. For the bi-crystalline specimen, the intergranular fracture was determined by stress concentration due to the difference in the strain between the deformed and undeformed crystals.

Intermetallic compounds have potential applications in a wide variety of structural and functional materials because of their unique characteristics, such as inverse temperature dependence of strength, superior resistance to oxidation and semiconducting behaviour. However, the use of intermetallics in product processing is currently limited because of their brittle nature, which is due to the limited number of slip systems in their crystal structure. As an illustration, a NiAl polycrystalline alloy, in which the $\{011\}\ \langle 100\rangle$ slip systems dominate, exhibits intergranular fracture, leading to significantly low ductility at room temperature. Thus far, improvements in the ductility of intermetallics have been accomplished by grain boundary strengthening with alloying elements, removal of impurities [1,2], and by providing deformable secondary phases [3,4]. The addition of Cr and Mn to a NiAl alloy affected its slip behaviour by increasing the number of activated slip systems, thus maintaining continuous plastic deformation even in the polycrystalline alloy [5].

The FeCo intermetallic alloy, which consists of a B2-type ordered structure based on a body centred cubic structure, is of interest because it possesses superior soft magnetic properties with a high saturation magnetic flux density [6]. However, this alloy exhibits extremely low workability due to the onset of intergranular fracture. Several studies have been conducted to improve the ductility of such alloys through grain boundary strengthening and microstructural control via addition of a third element [7–14]. However, the addition of alloying elements and consequent precipitation of secondary phases degrades the original magnetic properties of the alloy [6,11,12]. Therefore, it is necessary to prevent intergranular fracture without the help of additional elements. Comprehending the plastic behaviour of individual grains of the FeCo alloy may provide avenues for enhancing the mechanical properties of the alloy.

Compression tests employing single-crystalline (SC) specimens have revealed that the $\{1\bar{1}0\}\ \langle 111\rangle$ slip is primarily activated in an ordered FeCo alloy [15]. Unfortunately, plastic behaviour observed during compression testing cannot account for the brittle nature of the polycrystalline FeCo alloy as such a brittle fracture is not expected under compression conditions. Conventional mechanical testing is also inadequate for analysing the small deformation that occurs prior to intergranular fracture. In the present study, small SC and bi-crystalline (BC) specimens with defined crystallographic orientations are subjected to micro-tensile testing. The dimensions of the specimens are chosen to be on the scale of several tens of micrometres, where the so-called 'size effect' [16] and the effect of a damage layer due to focused ion beam (FIB) fabrication [17] is not significant.

An Fe–49.3 at.% Co alloy, prepared by arc melting under Ar atmosphere, was used as the target analyte. The thus-produced button ingot of this alloy was encapsulated in a silica tube with Ar gas and homogenised at a temperature of 1373 K for 3.6 ks. In a previous study [7], the long range order parameter, S, indicating the degree of order, was measured to be ~0.85 for the FeCo alloy obtained at the same heat-treatment temperature as the present study did. To obtain coarse grains, the encapsulated ingot was heated to a temperature of 873 K, where it was held for 86.4 ks. The sample was thinned to a thickness of <30 μm by mechanical grinding with emery papers and diamond

* Corresponding author.
E-mail address: mine@msre.kumamoto-u.ac.jp (Y. Mine).

http://dx.doi.org/10.1016/j.scriptamat.2017.08.012
1359-6462/

slurry. The crystal orientation was determined via electron back scatter diffraction (EBSD) measurement using TexSEM Laboratory orientation imaging microscopy (OIM) software (v.7.1.0). Tensile specimens (SC and BC) with gauge section dimensions of ~$20 \times 20 \times 50\ \mu m^3$ were fabricated by using an FIB. Two SC specimens were prepared: (a) a soft orientation (SCS) specimen, where the loading direction (LD) was nearly parallel to the [123] axis, and (b) a hard orientation (SCH) specimen, where the LD was nearly parallel to the [111] axis. The highest Schmid factors for the $\{1\bar{1}0\}\ \langle 111\rangle$ slip systems of SCS and SCH are 0.477 and 0.284, respectively. The BC specimen was composed of soft and hard crystals, denoted as BCS and BCH, respectively. The grain boundary of the BC specimen was arranged nearly perpendicular to the LD. Microtensile tests were performed at a displacement rate of 0.1 $\mu m\ s^{-1}$, corresponding to an initial strain rate of $2.0 \times 10^{-3}\ s^{-1}$, at room temperature, under laboratory atmosphere. For dynamic strain measurement during testing, the gauge section was monitored using an optical microscope. For comparison, a polycrystalline (PC) tensile specimen with gauge section dimensions of ~$0.4 \times 0.4 \times 1.0\ mm^3$ was prepared via electro-discharge machining, where the damage layer was removed by grinding with emery paper. The average grain size was ~230 μm for the PC specimen. The PC specimen was subjected to tensile testing at an initial strain rate of $1.67 \times 10^{-3}\ s^{-1}$.

Fig. 1 shows the stress–strain curves for the SCS, SCH, BC, and PC specimens and the fracture morphology of the BC specimen. The stereographic triangle in Fig. 1a indicates the initial LDs of the SC and BC crystals. Both SC specimens exhibited a high ultimate tensile strength of $\sigma_B = 600$–700 MPa and a large elongation to failure of $\varepsilon_F = 30$–40%. These values are significantly higher than those ($\sigma_B = 330$ MPa and $\varepsilon_F = 3.2\%$) obtained for the millimetre-long PC specimen. Because the tensile test revealed intergranular fracture and cleavage features for the PC specimen, these brittle fracture modes could counteract the ductile nature of the FeCo crystals. The yield stress, which is defined as the stress at 0.2% plastic strain, was 206 MPa for SCS and 357 MPa for SCH. Although no slip traces were observed at the onset of yielding, the critical resolved shear stress (CRSS) values were determined to be 98 MPa and 101 MPa for SCS and SCH, respectively, assuming that the $\{1\bar{1}0\}\ \langle 111\rangle$ slip system, exhibiting the highest Schmid factor, was activated. These values are consistent with each other. In contrast, the work-hardening behaviour was different in the two orientations. The SCS specimen exhibited two-step work-hardening behaviour before the flow stress reached a peak. For the SCH specimen, significant work-hardening occurred just after the onset of yielding. It is inferred that for the SCS specimen, the low work-hardening regime due to easy slip gliding is followed by a steeper work-hardening regime associated with occurrence of multiple slip gliding after crystal rotation. In the SCH specimen, the six $\{1\bar{1}0\}\ \langle 111\rangle$ slip systems were nearly equivalently oriented. This resulted in the activation of several slip systems just after the onset of yielding, resulting in a significantly high work-hardening rate. Although it is not easy to evaluate elastic anisotropy quantitatively from the present experimental results with a number of scattering data points, the slopes of stress–strain curves during elastic deformation (apparent elastic modulus) of $\langle 111\rangle$ and $\langle 123\rangle$ loadings are different. While this difference suggests that FeCo is elastically anisotropic as similar to the other B2-type intermetallic alloys [18], further experimental measurements are necessary to discuss elastic properties of FeCo quantitatively.

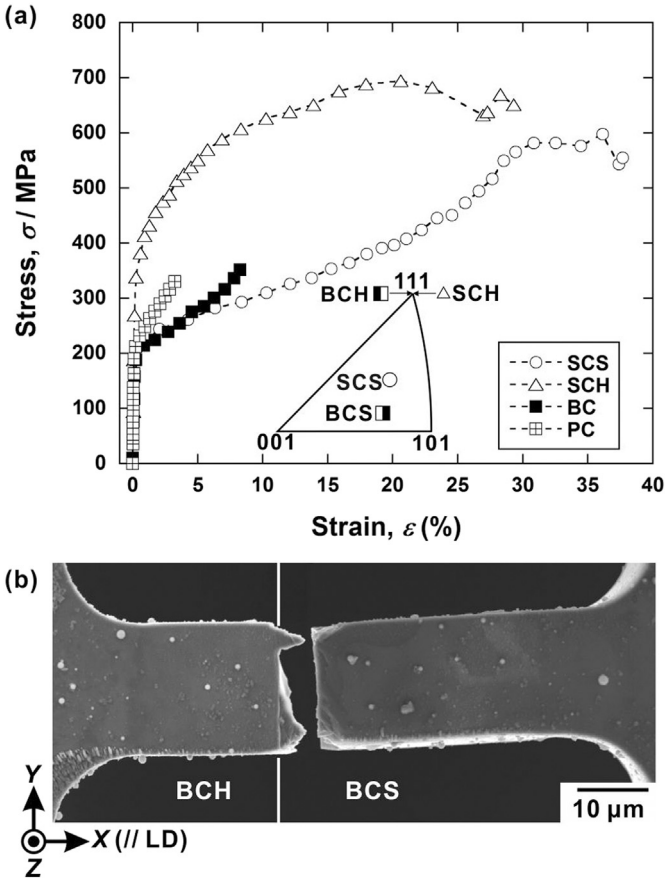

Fig. 1. (a) Stress–strain curves for the SCS, SCH, BC, and PC specimens and (b) SEM image of BC after failure.

The BC specimen started to yield at a stress of ~200 MPa and peak stress failure occurred at ~360 MPa (Fig. 1a). Yielding occurred in the BCS region, where the highest Schmid factor of the $\{1\bar{1}0\}\ \langle 111\rangle$ slip was 0.494, followed by interface boundary separation without any plastic deformation in the BCH region (Fig. 1b). Assuming that yielding occurred via activation of the primary slip system in the BCS region, the CRSS was determined to be 98 MPa, which is close to the values obtained for both SC specimens. Therefore, it is assumed that fracture occurs due to local strain accumulation at the interface after slip activation in the soft orientation grains.

A crystal plasticity finite element method (CPFEM) with a rate-dependent large strain crystal plasticity constitutive model [19] was used to investigate inhomogeneous deformation near the grain boundary in the BC specimen. The slip rate of the slip system i is calculated as:

$$\dot{\gamma}^{(i)} = \dot{\gamma}_0\ \mathrm{sgn}\left(\tau^{(i)}\right)\left|\frac{\tau^{(i)}}{g^{(i)}}\right|^{1/m}, \tag{1}$$

where $\dot{\gamma}_0$ is the reference slip rate, m is the strain sensitivity parameter; $\tau^{(i)}$ and $g^{(i)}$ are the resolved shear stress and reference stress for slip system i, respectively. The following evolution equation was used to calculate the evolution of $g^{(i)}$.

$$\dot{g}^{(i)} = \sum_{j=1} \Omega^{(ij)} h \left|\dot{\gamma}^{(j)}\right|, \tag{2}$$

where h is the strain hardening rate for the slip system i. In Eq. (2), $\Omega^{(ij)}$ is the interaction matrix describing latent-hardening between slip systems i and j. All of the diagonal components ($i = j$) of $\Omega^{(ij)}$ are unity. The $\{1\bar{1}0\}\ \langle 111\rangle$ slip system was used for the deformation modes.

For elastic property, isotropic elasticity is assumed with the Young's modulus $E = 188$ GPa and Poisson's ratio $\nu = 0.31$ referring the past experimental measurement [20]. Although a theoretical prediction of elastic anisotropy of FeCo has been reported [21], there is no publication showing experimental values of elastic constants as far as the authors know. Assuming that the strain rate sensitivity is similar to that of steels, $m = 0.02$ was used. The initial reference stress $g^{(i)}$ for the $\{1\bar{1}0\}\ \langle 111\rangle$ slip was set to 99.5 MPa, which was determined herein from a single-crystal experiment.